Local Work Function of Pt Clusters Vacuum-Deposited on a TiO_2 Surface

Akira Sasahara,*,†,‡ Chi Lun Pang,‡,§ and Hiroshi Onishi‡

Japan Science and Technology Agency, Kawaguchi, Saitama 332-0012, Japan, and Department of Chemistry, Faculty of Science, Kobe University, Nada-ku, Kobe 657-8501, Japan

Received: June 13, 2006

Surface topography and work function maps were simultaneously obtained for Pt-evaporated titanium dioxide (TiO_2) surfaces by using a Kelvin probe force microscope (KPFM). Platinum clusters with diameters of 2−3 nm and heights of 0.2−0.4 nm were obtained on rutile TiO_2(110)-(1 × 1) surfaces. The work function on the Pt clusters was smaller than that on the surrounding TiO_2 surface. With the assumption that the work function was perturbed by electric dipole moments created at the Pt−TiO_2 interface, the work function decrease indicates that dipole moments were created at the interface and directed toward the vacuum. Such dipole moments can be formed by electron transfer from the originally neutral Pt atoms to the Ti cations exposed on the (1 × 1) surface. A simple model is constructed by assuming a uniform dipole moment per unit interface area. Using this model, the size-dependent perturbation of the work function can be interpreted. The electrostatic potential is more perturbed above the Pt clusters with a larger interface area since the number density of dipole moments is equal to that of the Ti cations and is uniform. A similar correlation between the work function decrease and interface area was observed for the clusters formed on terraces and on step edges. The work function maps showed no peculiar contribution for Ti atoms exposed at the step edges. Vacuum annealing caused a considerable change in the work function on the clusters. The work function was decreased on some clusters relative to the TiO_2 substrate, while it increased on the other clusters. The atomistic structure of the interface may be modified upon annealing, thus perturbing the electron transfer across the interface.

Introduction

Loading small amounts of transition metals on metal oxide supports leads to catalysts which can attain high yields and selectivities.[1] In such catalysts, nanometer-sized metal clusters are often identified as the active components. Catalytic reactions, redox reactions in particular, are accompanied by electron transfer between adsorbates and catalysts. Investigating the electron distribution on a metal-on-oxide system therefore offers a route to elucidate the role of electron transfer in supported catalysts which could ultimately allow the identification of active clusters, leading to a precise understanding of catalysis.

Platinum-loaded TiO_2 finds many applications in catalysis including being a representative photocatalyst. It is thought that electrons excited in TiO_2 by UV irradiation are injected into the nanometer-sized Pt clusters, thereby promoting reduction reactions on the cluster surface.[2] The photoelectron injection should be sensitive to the local charge distribution over a Pt-deposited TiO_2 surface. In the present study, the local work function on Pt-evaporated TiO_2 surfaces was measured with nanoscale spatial resolution. Electron transfer between individual Pt clusters and the TiO_2 substrate is examined on the basis of the distribution of the local work function.

We employed a (110) oriented rutile TiO_2 as the substrate as it gives an atomically flat surface convenient for microscope analysis.[3,4] Figure 1 shows a model of the nonreconstructed (1 × 1) structure of TiO_2(110). Bridging O atoms form rows which extend along the [001] direction. Between the rows of O atoms, 5-fold-coordinated Ti atoms are exposed and also align in the [001] direction. Three-dimensional growth of vacuum-deposited Pt has been concluded on the (1 × 1) surface on the basis of peak intensity analysis of low-energy ion scattering spectra[5] and X-ray photoelectron spectra.[6] These conclusions were supported by subsequent scanning tunneling microscope images.[7] It has been assumed from the photoelectron spectra that electron transfer does not occur between the deposited Pt and the substrate. The absence of a zero-cutoff energy shift suggested an undetectable perturbation of the work function.[6] A shift of Pt 4f peaks to higher binding energy at submonolayer coverage

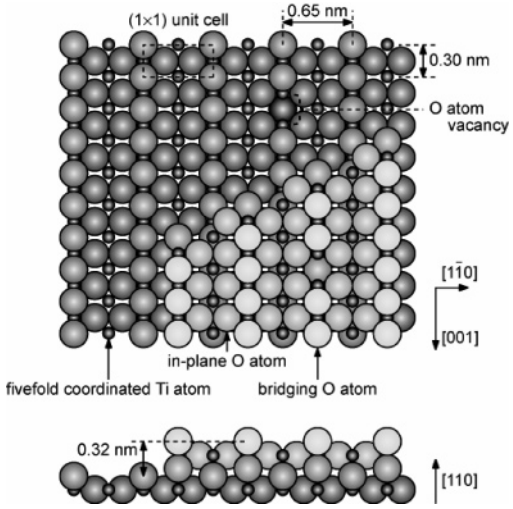

Figure 1. A ball model of the TiO_2(110)-(1 × 1) surface including monatomic steps. Small and large spheres represent Ti and O atoms, respectively. The O atoms are shaded according to their depth.

* Author to whom correspondence should be addressed. E-mail: sasahara@kobe-u.ac.jp.

† Japan Science and Technology Agency.

‡ Kobe University.

§ Present address: London Centre for Nanotechnology and Department of Chemistry, University College London, 20 Gordon Street, London WC1H 0AJ, United Kingdom.

10.1021/jp063665h CCC: $33.50
Published on Web 08/17/2006

was assigned to a less-effective screening of the positive holes created by photoemission.[5,6]

Our work function measurements were conducted by using a Kelvin probe force microscope (KPFM)[8] which provides both the surface topography and the lateral distribution of work function of a sample surface. The KPFM represents an extension of the noncontact atomic force microscope (NC-AFM).[9] The NC-AFM is a probe microscope which can obtain atom-scale images of sample surfaces by detecting atomic forces. A cantilever with a tip at one end is oscillated at its resonant frequency (f_0). When the sample exerts an attractive force on the tip, the oscillation frequency changes so that the attractive force can be monitored as a frequency shift (Δf). The tip−sample distance is regulated so that Δf is constant. In the KPFM measurement, the cantilever is additionally used as a reference electrode of a Kelvin probe so that the contact potential difference at each point in the scan is measured simultaneously with the topography. During KPFM measurement, the sample bias voltage (V_s) is modulated by an AC voltage to derive an electrostatic interaction that originated from the contact potential difference. Like the NC-AFM, the lateral resolution of the obtained work function map can also reach the atomic scale.[10−13] Work function is defined on materials of a macroscopic size. A KPFM detects the local contact potential difference between the tip and sample. The authors use "work function" in this manuscript to unequivocally show the direction of the potential shift observed.

Experimental Section

Experiments were carried out by using an ultrahigh vacuum microscope (JSPM-4500A, JEOL) equipped with a KPFM driver (TM-Z50241, JEOL), Ar^+ sputtering gun (IG35, OCI), and low-energy electron diffraction optics (BDL600, OCI). The base pressure of the microscope chamber was 2×10^{-8} Pa. A conductive Si cantilever (NSC12, Mikro Masch) with f_0 of 300 kHz and spring constant of 14 N/m was used as a probe. The tip was occasionally sputtered with an Ar^+ beam to remove contaminants. During the acquisition of simple NC-AFM topography images, a constant V_s was applied to cancel the average contact potential difference between the tip and sample. During KPFM measurements, V_s was modulated with an ac voltage (2 V, 2 kHz).

A mechanically polished TiO_2(110) wafer ($7 \times 1 \times 0.3$ mm^3, Shinko-sha) was clamped against a Si heater. The (1×1) surface was prepared by cycles of Ar^+ sputtering and annealing at 1100 K in a vacuum. The temperature of the sample was monitored with an infrared pyrometer (TR630, Minolta), and it was possibly overestimated due to the incomplete contact between the TiO_2 and Si wafers. After cooling to room temperature, the sputter-annealed surface was exposed to a resistively heated Pt wire (99.98%, Nilaco) which was outgassed beforehand. The distance between the sample wafer and Pt source was about 60 mm, and the increase of pressure during evaporation was less than 8×10^{-8} Pa. The amount of Pt dosed was controlled by changing the exposure time.

All images were presented without filtering. Cross-section analysis was carried out on images filtered with a nine-point median operation. The geometrically higher areas are presented brighter in topography, and areas with a larger work function are presented brighter in the work function maps.

Results and Discussions

Prior to work function mapping, we examined the surfaces in the simple NC-AFM mode which readily gives atom-scale topography. Figure 2a shows images of the TiO_2(110)-(1×1) surface. The surface consists of flat terraces separated by monatomic steps. On the terraces, the rows of O atoms are observed as bright lines extending in the [001] direction. Additionally, individual O atoms are resolved as bright spots in the narrow-scan image inset in Figure 2a. The depressions interrupting the O atom rows (indicated by arrows) are vacancies where O atoms have been removed. These features are consistent with those previously reported.[14] The number density of O vacancies is 0.027 nm^{-2}. Figure 2b,c show the topography of the (1×1) surfaces following exposure to the heated Pt wire for 10 and 120 min. Since the number of bright particles increases with exposure time, we assigned them to Pt clusters. The number density of O vacancies in the image of Figure 2b is 0.024 nm^{-2}. This density is comparable to the clean surface in Figure 2a, indicating no preference for nucleation at O vacancies. This contrasts with observations of the evaporation of Au on TiO_2(110)[15] where gold atoms were proposed to be mobile on the (1×1) surface at room temperature, stabilizing at O vacancies. The Pt adatoms are probably less mobile than the Au adatoms and therefore nucleated randomly over the surface. The image in Figure 2d shows the topography of the surface which has been exposed to the Pt source for 10 min and then annealed for 3 min at 830 K. In the annealed sample, the size of the clusters increases from their size in the unannealed sample. The number density of the O vacancies increased to 0.053 nm^{-2}. It is likely that annealing enhances the mobility of the Pt clusters and adatoms so that they can find low energy positions at step edges and perhaps also at O vacancies. Oxygen vacancies can, on the other hand, be formed during vacuum annealing which probably accounts for their observed increase.

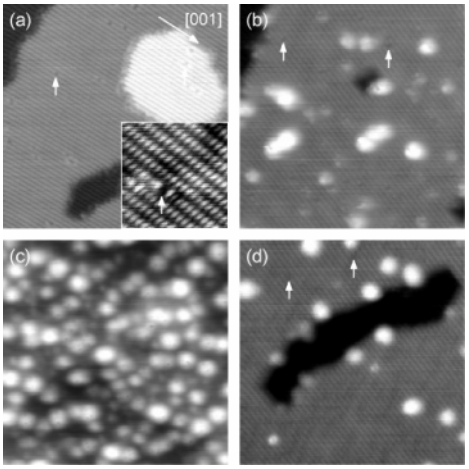

Figure 2. NC-AFM topographic images of the TiO_2(110)-(1×1) surfaces exposed to Pt vapor for (a) 0, (b) 10, and (c) 120 min. The surface in (d) was annealed at 830 K in a vacuum after Pt evaporation of 10 min. Some of the O vacancies are marked by arrows. Image sizes are 30×30 nm^2 (inset in (a): 5×5 nm^2). (a) Frequency shift (Δf): −64 Hz (inset: −136 Hz), sample bias voltage (V_s): +0.6 V (inset: +0.9 V), peak-to-peak amplitude of the cantilever oscillation (A_{p-p}): 6.0 nm (inset: 6.0 nm); (b) Δf: −68 Hz, V_s: +1.2, A_{p-p}: 6.8 nm; (c) Δf: −25 Hz, V_s: +0.4, A_{p-p}: 6.7 nm; (d) Δf: −142 Hz, V_s: +1.0, A_{p-p}: 6.5 nm.

Figure 3a,b shows topography and work function maps of the TiO_2 surface after exposure to Pt vapor for 10 min. In the topography image shown in Figure 3a, the Pt clusters are resolved together with the O atom rows on the terraces. As shown in the histograms in Figure 3c, the height and diameter of Pt clusters maximize at around 0.28 and 3.6 nm, respectively and the average height and diameter of the clusters are 0.30 and 3.20 nm, respectively. The simultaneously obtained work

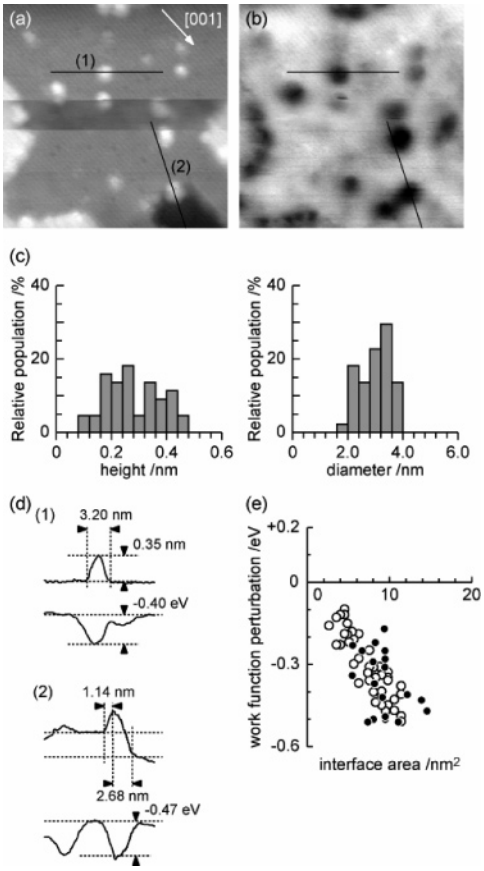

Figure 3. Simultaneously obtained (a) topography and (b) work function maps of the Pt-evaporated TiO_2 surface. Image size: 30×30 nm^2, Δf: -58 Hz, A_{p-p}: 6.8 nm, scanning speed (v_s): 1.7 s/line. (c) Distribution of the heights and diameters of the Pt clusters formed on the terraces. (d) Cross sections obtained along the lines in images (a) and (b). (e) Deviation of work function on the Pt clusters from that on the TiO_2 surface plotted as a function of the cluster$-TiO_2$ interface area. Open and filled circles are obtained on the Pt clusters formed on terraces and steps edges, respectively.

function map in Figure 3b reveals that the work function on the Pt clusters is smaller than that on the surrounding TiO_2 surface. On a Pt-free, clean TiO_2(110) surface, work function perturbations on the terraces and at the steps were within several 10 mV.[16] Therefore the local work function decrease in this study must be due to the presence of the Pt clusters.

We attribute the work function perturbation to electric dipoles formed at the interface between the Pt and the substrate. The work function decrease is caused by a dipole moment directed from the substrate to the vacuum. Therefore the work function decrease indicates transfer of electrons from the Pt clusters to the TiO_2 substrate. Originally neutral Pt atoms donate electrons to the positively charged surface Ti atoms. In our previous KPFM study,[10] the work function was shown to locally decrease on Pt adatoms adsorbed on the Ti atom rows of the TiO_2(110)-(1×1) surfaces. Electron transfer from Pt clusters to TiO_2 supports has been proposed previously in studies of Pt-loaded TiO_2 catalysts.[16,17] In electron magnetic resonance spectra, two signals assignable to the Pt^+ and Ti^{3+} were observed, indicating that the oxidation of Pt atoms and reduction of Ti^{4+} cations is caused by electron transfer from the Pt.[17] The number of unfilled Pt 5d states estimated from X-ray absorption near edge fine structure was larger than that of a reference Pt foil. This was also attributed to electron donation from the Pt cluster to the TiO_2 support.[18] The electron transfer to the TiO_2 substrate would

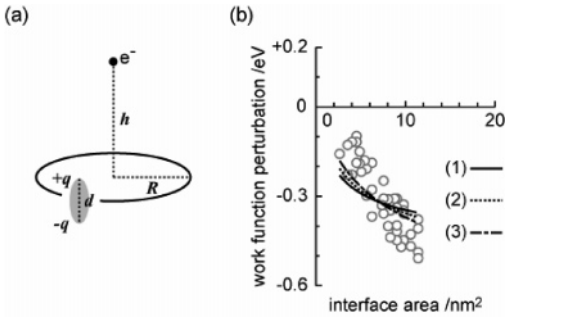

Figure 4. (a) A model for calculation of the electrostatic potential above the Pt clusters. (b) The $V-S$ curves fitted to the experimentally obtained work function decrease (open circles) assuming (1) $h = 0.5$, (2) $h = 0.7$, and (3) $h = 1.0$ nm.

be inherent to the nanometer-sized clusters. In the previous photoelectron spectroscopy studies on the TiO_2(110) surfaces,[5,6] the amount of evaporated Pt may have been higher and the clusters larger than those examined in our study.

The work function decrease on the Pt clusters is well-correlated with the area of the cluster$-TiO_2$ interfaces. The diameters of the interfaces were determined from the cross sections obtained in the topography as shown in Figure 3d. As for the clusters formed at the step edges, two semicircular areas were estimated for each terrace and added to the trapezoid interface area of the step. Figure 3e shows the work function decreases on the clusters plotted as a function of the interface area. The work function on the clusters decreases as the interface area increases. This interface area dependence was similar whether the clusters were on terraces or at step edges. One may expect that the step edges affect the work function on the clusters because the Ti atoms at the step edges are coordinated to four or fewer O atoms[19] and should be less positively charged than the 5-fold-coordinated Ti atoms on the terraces. Since the number of Ti atoms which are at step edges and included in the cluster$-TiO_2$ interface is small compared with the number of Ti atoms exposed on a terrace, the work function decrease is insensitive to the step edges. When the diameter of the cluster is 2 nm, the number of 5-fold-coordinated Ti atoms included at the cluster$-TiO_2$ interface is 16. The line density of the 4-fold-coordinated Ti atoms along the $<1\bar{1}1>$ steps, which are the predominant steps on the (1×1) surface, is 1.4 nm^{-1}, and the number of 4-fold Ti atoms is estimated to be 1 or 2.

Our assumption that electrons transfer from Pt to Ti atoms explains the size dependence of the work function decrease. Figure 4a shows a model of the cluster$-TiO_2$ interface. Dipoles which are composed of charges of $\pm q$ separated by a distance, d, are placed with a number density of ρ in a circular interface with a radius of R. The electrostatic potential, V, at the point separated from the center of the circle by h is given by

$$V = \frac{1}{4\pi\epsilon_0}\int_0^R \frac{2\pi r\rho q}{\sqrt{r^2+h^2}}dr - \frac{1}{4\pi\epsilon_0}\int_0^R \frac{2\pi r\rho q}{\sqrt{r^2+(h+d)^2}}dr$$

$$= \frac{\rho q}{2\epsilon_0}\{(\sqrt{R^2+h^2}-h) - (\sqrt{R^2+(h+d)^2}-(h+d))\}$$

$$= \frac{\rho q}{2\epsilon_0}\left\{\left(\sqrt{\frac{S}{\pi}+h^2}-h\right) - \left(\sqrt{\frac{S}{\pi}+(h+d)^2}-(h+d)\right)\right\} \quad (1)$$

The value of V obtained using eq 1 shows the work function decrease as a function of the area of the circle, S. h represents

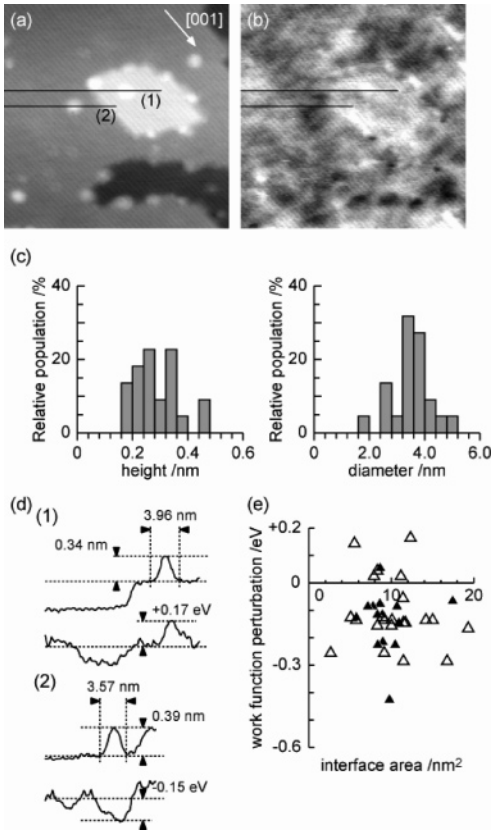

Figure 5. Simultaneously obtained (a) topography and (b) work function maps of the Pt-evaporated TiO_2 surface after annealing in a vacuum at 830 K for 1 min. Image size: 30×30 nm^2, Δf: -58 Hz, A_{p-p}: 6.8 nm, v_s: 1.7 s/line. (c) Distribution of the heights and diameters of the Pt clusters formed on the terraces. (d) Cross sections obtained along the lines in images (a) and (b). (e) Deviation of work function on the Pt clusters from that on the TiO_2 surface plotted as a function of the cluster$-TiO_2$ interface area. Open and filled triangles are obtained on the Pt clusters formed on terraces and steps edges, respectively.

the minimum tip−sample distance in the KPFM measurement and is generally 1 nm or less. The solid line (1), dotted line (2), and broken line (3) in Figure 4b are the $V-S$ curves fitted to the experimental data obtained for the clusters on the terraces for $h = 0.5$, 0.7, and 1.0 nm, respectively. The number density of the surface Ti atoms, 5.1 nm^{-2}, was used as ρ. d was estimated and fixed to be 0.20 nm from the sum of the ionic radius of Ti^{4+} and the metallic radius of Pt, 0.061 and 0.14 nm, respectively.[20] q was optimized by the curve-fitting procedure for each value of h used, giving $q = 0.09 \times 10^{-19}$, 0.1×10^{-19}, and 0.13×10^{-19} C for $h = 0.5$, 0.7, and 1.0 nm, respectively. These values for q represent possible values for electron transfer between the Pt and Ti atoms. The order of transferred charge, 0.1 electron or less per Pt atom, appears to be reasonable.

To estimate the electron transfer more rigorously, the effect of the shape of the tip apex has to be taken into account. Numerical simulations[21,22] showed that contact potential difference measured by KPFM is sensitive to the tip radius. Another issue to be refined in a future simulation is the oscillated tip−surface distance. The tip was oscillated with a peak-to-peak amplitude of 5 nm in the experiments, while h was fixed at desired numbers in the simulation. The electrostatic potential is a function of the tip−surface distance. The experimentally observed potential should be a weighted average of the distance-dependent potential over one oscillation cycle. How weighted? The gradient of the electrostatic force is minimized to find the local contact potential difference in the frequency-modulated KPFM.[21] This gradient is proportional to the second derivative of the tip−surface capacitance and hence enhanced with small tip−surface distances. The potential at minimum distances, instead of the weighted average, was estimated in the simulation of Figure 4.

We have also examined the effect of vacuum annealing on the work function of the Pt clusters. Figure 5a,b shows the topography and work function maps of the (1×1) surface exposed to Pt vapor for 10 min and annealed subsequently at 830 K for 1 min. The average height and diameter of the clusters on the terraces increases slightly to 0.31 and 3.70 nm, respectively. Although the growth of clusters was minimal, the work function map changed dramatically following annealing. While some clusters show a higher work function than that of the surrounding TiO_2 surface, as shown in cross section (1) of Figure 5d), other clusters still show a work function decrease, as shown in cross section (2). As illustrated in Figure 5e, the overall work function decrease is suppressed and the correlation between work function perturbation and interface area is lost.

One possible cause for the change of the work function on the Pt clusters is a rearrangement of the atoms at the cluster−TiO_2 interface. The electron transfer should be dependent on atom−atom distances and their coordination numbers. Indeed, the work function has recently been shown to be sensitive to the adsorption sites of Pt adatoms on the (1×1) surface. The work function decrease on single Pt adatoms adsorbed on the Ti atom rows was 0.24 eV compared with 0.26 eV for Pt adatom in O vacancies.[10] In the present study, intermixing of the Pt and Ti atoms at the interface may lead to formation of the dipole moments directed in the opposite direction. Encapsulation of the clusters by TiO_x species seems less likely. It is well-known that nanometer-sized metal clusters can be covered by TiO_x layers when metal-loaded TiO_2 is annealed in reducing conditions.[23,24] However, the heights and diameters of the clusters before and after annealing were comparable and hence encapsulation seems unlikely.

Summary

The KPFM measurements of the Pt-evaporated $TiO_2(110)$ surfaces showed that the work function on the Pt clusters decreases as a function of the area of the cluster−TiO_2 interface. The work function decrease was explained by assuming that electric dipoles were formed at the cluster−TiO_2 interfaces by electron transfer from the Pt atoms to the surface Ti atoms. Vacuum annealing caused further work function perturbation on the clusters, which was possibly due to the change of atom configuration at the cluster−TiO_2 interface. We believe our results represent a significant advance toward understanding the role of electron transfer in the catalytic behavior of the Pt/TiO_2 system.

Acknowledgment. The present work was supported by Core Research for Evolutional Science and Technology (CREST) from the Japan Science and Technology Agency (JST) and Grant-in-Aid for Scientific Research in Priority Area "Molecular Nano Dynamics" from Ministry of Education, Culture, Sports, Science and Technology. C.L.P. was supported by the Japan Society for the Promotion of Science (JSPS) Fellowship.

References and Notes

(1) Gates, B. C. *Chem. Rev.* **1995**, *95*, 511.
(2) Linsebigler, A. L.; Lu, G.; Yates, J. T., Jr. *Chem. Rev.* **1995**, *95*, 735.
(3) Diebold, U. *Surf. Sci. Rep.* **2003**, *48*, 53.

(4) Henrich, V. E.; Cox, P. A. *The Surface Science of Metal Oxides*; Cambridge University Press: New York, 1994; p 44.
(5) Steinrück, H. P.; Pesty, F.; Zhang, L.; Madey, T. E. *Phys. Rev. B* **1995**, *51*, 2427.
(6) Schierbaum, K. D.; Fischer, S.; Torquemada, M. C.; de Segovia, J. L.; Román, E.; Martín-Gago, J. A. *Surf. Sci.* **1996**, *345*, 261.
(7) Gan, S.; Liang, Y.; Baer, D. R.; Grant, A. W. *Surf. Sci.* **2001**, *475*, 159.
(8) Nonnenmacher, M.; O'Boyle, M. P.; Wickramasinghe, H. K. *Appl. Phys. Lett.* **1991**, *58*, 2921.
(9) *Noncontact Atomic Force Microscopy*; Morita, S., Wiesendanger, R., Meyer E., Eds.; Springer: Berlin, 2002.
(10) Sasahara, A.; Pang, C. L.; Onishi, H. *J. Phys. Chem. B* **2006**, *110*, 13453.
(11) Sasahara, A.; Uetsuka, H.; Onishi, H. *Jpn. J. Appl. Phys.* **2004**, *43*, 4647.
(12) Okamoto, K.; Yoshimoto, K.; Sugawara, Y.; Morita, S. *Appl. Surf. Sci.* **2003**, *210*, 128.
(13) Kitamura, S.; Suzuki, K.; Iwatsuki, M.; Mooney, C. B. *Appl. Surf. Sci.* **2000**, *157*, 222.
(14) Fukui, K.; Onishi, H.; Iwasawa, Y. *Phys. Rev. Lett.* **1997**, *79*, 4202.
(15) Wahlström, E.; Lopez, N.; Schaub, R.; Thostrup, P.; Rønnau, A.; Africh, C.; Lægsgaard, E.; Nørskov, J. K.; Besenbacher, F. *Phys. Rev. Lett.* **2003**, *90*, 026101.
(16) Sasahara, A.; Uetsuka, H.; Onishi, H. *Surf. Sci.* **2003**, *529*, L245.
(17) Salama, T. M.; Hattori, H.; Kita, H.; Ebitani, K.; Tanaka, T. *J. Chem. Soc., Faraday Trans.* **1993**, *89*, 2067.
(18) Short, D. R.; Mansour, A. N.; Cook, J. W., Jr.; Sayers, D. E.; Katzer, J. R. *J. Catal.* **1983**, *82*, 299.
(19) Diebold, U.; Lehman, J.; Mahmoud, T.; Kuhn, M.; Leonardelli, G.; Hebenstreit, W.; Schmid, M.; Varga, P. *Surf. Sci.* **1998**, *411*, 137.
(20) *CRC Handbook of Chemistry and Physics*; Lide, D. R., Ed.; CRC Press: Boca Raton, FL, 2004.
(21) Zerweck, U.; Loppacher, C.; Otto, T.; Grafström, S.; Eng, L. M. *Phys. Rev. B* **2005**, *71*, 125424.
(22) Ono, S.; Takahashi, T. *Jpn. J. Appl. Phys.* **2004**, *43*, 4639.
(23) Dulub, O.; Hebenstreit, W.; Diebold, U. *Phys. Rev. Lett.* **2000**, *84*, 3646.
(24) Tauster, S. J.; Fung, S. C.; Baker, R. T. K.; Horsley, J. A. *Science* **1981**, *211*, 1121.